Indian Journal of Pure & Applied Physics
Vol. 53, March 2015, pp. 160-168

Design, analysis and multipacting studies of 650 MHz, β=0.61 superconducting *RF* cavity

Sumit Som*, S Seth, A Mandal & S Ghosh

Variable Energy Cyclotron Centre, Kolkata 700 064, India

*E-mail: ssom@vecc.gov.in

Received 24 July 2014; revised 14 November 2014; accepted 8 January 2015

With the advancement of superconducting *RF* technologies in the past few decades, the superconducting *RF* (SCRF) cavities with high accelerating gradient have become the technology of choice for the future energy frontier linear accelerators. In India, DAE laboratories and other institutions are now actively involved in research and development activities on SCRF cavities and associated technologies for the proposed future high current, high energy proton linear accelerators like Spallation Neutron Source (SNS)/Accelerator Driven Sub-critical System (ADSS) and also for the Project-X program of FERMILAB, under Indian institutions- Fermilab collaboration (IIFC). This paper describes about the related work on the *RF* design of the single and five-cell SCRF cavities to be operated at 650 MHz frequency with velocity factor (β) of 0.61. The 2D and 3D simulations of the elliptical shape cavity with emphasis on re-entrant and elliptical shapes have also been studied. The comparative study of two different shapes of the above cavities has been carried out with regard to the dependence of peak surface electric and magnetic field on various geometrical parameters of the said cavity. The design philosophy of end-cell of the cavity has also been discussed. The optimized cavity has also been compared with existing designs of similar cavities done by Jefferson Lab (JLab) and Fermilab, USA. The preliminary 2D study of Multipacting phenomenon for the cavity has also been touched upon.

Keywords: Superconducting, *RF*, Re-entrant, Cavity, Multipacting, Linac

1 Introduction

The field of superconducting accelerating structures is separated into three distinct velocity regions. The low-velocity (β≤0.2), medium velocity (β ~0.2 to 0.65) and high-velocity (β~0.65 to 1) structures are practically realized in various laboratories in the world. The medium-β superconducting accelerators are operated in different categories, like high-current continuous-wave (CW), high-current pulsed, or low-to-medium current CW. The operation is limited by practical considerations, up to a gradient of 20 MV/m. In CW applications, operating gradients are limited by the load to the cryogenic system. The high shunt impedance is often a more important objective than achieving high gradient in CW applications. In high current applications, the gradients are limited by the capability of the fundamental power couplers (FPC). In low current applications, accelerating gradients are limited by the *RF* power required for field control.

The high accelerating gradient SCRF cavities are the only choice for the energy frontier accelerators. A lot of progress on achieving higher and higher gradient (E_{acc}) has been made by various laboratories around the world over the past few decades. The E_{acc} of a single-cell re-entrant shape cavities[1] made of fine-grain and large grain niobium have been reached up to the world record value of 59 MV/m at 1.3 GHz in Cornel University, USA for ILC and also a low-loss shape niobium cavity[2] of 53.5 MV/m at 1.3 GHz in KEK, Japan. It is well established that the peak surface electric field (E_{pk}), and peak surface magnetic field (B_{pk}) are the two deciding parameters to achieve the maximum accelerating gradient[3]. Both E_{pk} and B_{pk} increase proportionally as E_{acc}. However, it is desirable to minimize the ratios E_{pk}/E_{acc} and B_{pk}/E_{acc} both, which is a contradictory requirement. If one of them is reduced, the other one gets increased. So adequate optimization is necessary in the design. These ratios are solely determined by the cavity geometry[4]. Theoretically, there is no fundamental limit to E_{pk}, although field emission control is practically a challenging task[5]. But there is a hard limit[6] to B_{pk}. To achieve higher E_{acc}, the ratio B_{pk}/E_{acc} has to be minimized by optimizing the cavity geometry. The design optimization and analysis of β=0.61, 650 MHz, 5-cell elliptical shape superconducting *RF* linac cavity have been done at VECC, Kolkata. The effect of various geometric

parameters on different *RF* design parameters has been analyzed for the said cavity and the shape has been optimized using 2D SUPERFISH and 3D CST MICROWAVE STUDIO codes. The comparative study of *RF* design parameters for two types of cell shapes, re-entrant and non re-entrant has been discussed in the present paper. The simulation study of the probable multipacting problem has also been carried out.

2 *RF* Design

The elliptical shaped cell of the cavity consists of two elliptic arcs and, possibly, a straight line between them and thus the shape of an elliptical cavity (as shown in Fig. 1) is determined by geometric parameters[7] like cell length (*L*), equator radius (*D*/2), iris radius or aperture radius (R_{iris}), iris ellipse ratio (a/b), equator ellipse ratio (A/B), slope of the side wall (α) and the distance (*d*) measured from the iris plane. The main figures of merit for an elliptical-cell design of a superconducting *RF* cavity are E_{pk}/E_{acc}, B_{pk}/E_{acc}, geometric factor (G) and the ratio of shunt impedance to quality factor (R/Q).

Iris radius has very strong influence on the above mentioned merit values[8].With the decrease of R_{iris}, both the ratios E_{pk}/E_{acc} and B_{pk}/E_{acc} decrease, but the other two parameters *G* and R/Q increase[9]. By optimizing the value of geometric parameters, optimal merit values have been determined for 650 MHz, β=0.61, 5-cell elliptical cavity.

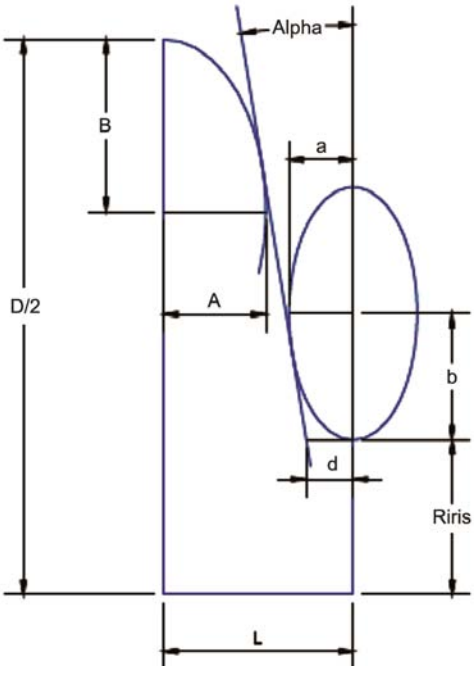

Fig. 1 — (1/4)th cell Geometry of elliptical shape cavity

2.1 Re-entrant and elliptical shape single-cell cavities

The two parameters, E_{pk}, B_{pk}, decide the achievable accelerating gradient (E_{acc}) in elliptical shape cavity. Both E_{pk} and B_{pk} increase proportionally as E_{acc}. The ratios E_{pk}/E_{acc} and B_{pk}/E_{acc} are determined solely by the cavity geometry. Traditionally, the cavity shape is optimized to reduce E_{pk}/E_{acc}, as the field emission increases with E_{pk}/E_{acc} and limits the value of accelerating gradient (E_{acc}). By proper surface treatment, field emission in a elliptical cavity can be reduced. But there is a fundamental limit to E_{acc} due to an intrinsic limit referred to as the *RF* critical magnetic field ($B_{critical,RF}$) on the surface of superconductor. To overcome this hard fundamental limit, the ratio B_{pk}/E_{acc} has to be reduced by changing the cavity shape and this leads to the re-entrant elliptical shape cavity (as shown in Fig. 2). Re-entrant cavities[10] have negative value of wall slope angle (α).

Besides the lower value of B_{pk}/E_{acc}, the other advantages of re-entrant shape are higher values of *G* and R/Q, thus resulting in less *RF* power dissipation on the cavity wall and smaller heat load on the cryogenic system. On the contrary, the value of E_{pk}/E_{acc} is somewhat higher[10] for re-entrant type of cavities.

The geometry or the shape of the cavity is determined by several parameters as discussed below. The cell length (*L*) determines the geometrical β value of the cavity from the following relation.

$$L = \frac{\beta\lambda}{2} \qquad ...(1)$$

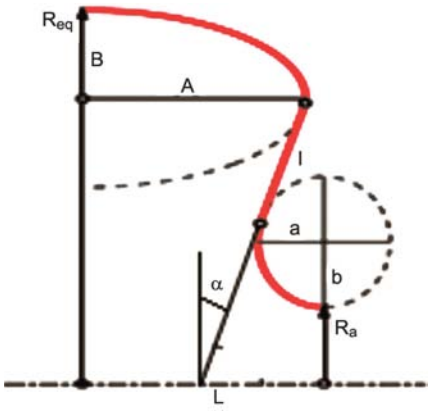

Fig. 2 — (1/4) th cell Geometry of of re-entrant shape

where λ is the wavelength of the electromagnetic wave.

The cell iris radius (R_{iris}) is primarily determined by the required cell-to-cell coupling. The wall slope angle (α) of the side wall and position (*d*) with respect to the iris plane can be set to achieve a trade-off between peak surface electric (E_{pk}) and magnetic (B_{pk}) fields with a minor effect on cell-to-cell coupling. The iris ellipse aspect ratio (a/b) uniquely affects the peak surface electric fields[4]. The equator ellipse aspect ratio (A/B) has very negligible effect on the *RF* parameters, but affects the mechanical behaviour of the cavity. The equator diameter or cell diameter (*D*) is varied for frequency tuning without affecting any electromagnetic or mechanical parameters of the cavity.

The tuning of the cell at the right frequency is done by varying the cell diameter (*D*) without changing any other independent parameters, namely, *L*, α, *d*, (a/b), (A/B). This is practically achieved by varying the equator ellipse parameters (A, B), but keeping their ratio (A/B) fixed. The distance between the ellipse centers, fulfilling the tangency condition, changes accordingly. In this manner, the cavity shape, uniquely determined by the six independent parameters, is not affected by the tuning procedure.

3 Results and Discussion

The comparative study on single-cell cavity with two different types of geometry, Re-entrant shape and elliptical shape for β=0.61, operating at 650 MHz has been carried out. The single-cell length of the cavity is 140.67 mm. and the iris diameter is 96 mm.

The simulations results are tabulated in Table 1 for elliptical and re-entrant shape single-cell cavities. It is observed from Table1 that the wall slope angle is negative (-10.48 degree) as compared to positive wall slope angle (2.38 degree) for the elliptical one. For the re-entrant cavity geometry, B_{pk}/E_{acc} value (4.525 mT/(MV/m)) is slightly improved (4%) with respect to that value (4.7172 mT/(MV/m)) for elliptical geometry. On the contrary, E_{pk}/E_{acc} value (3.085) for re-entrant cavity has been deteriorated by around 1.2% as compared to that value (3.048) for elliptical shape cavity. The higher values of geometric factor (G = 202.5) and the ratio of shunt impedance-to-quality factor (R/Q=63.2) have been achieved for re-entrant ones as compared to those values (G=192.9 and R/Q=58.6) for elliptical cavity. For the re-entrant shape cavity, as desired, the value of G is increased by around 5% and (R/Q) increased by 8% in comparison to the elliptical shape cavity. This simulation result confirms that *RF* power loss and heat load on cryogenic system will be less for re-entrant cavity.

To achieve the accelerating gradient of 17 MV/m, the energy (22.13 Joule) to be supplied to the re-entrant cavity is around 7.3% less than the energy (23.87 Joule) for the elliptical ones. However, there are some practical problems of cavity treatment like, high pressure water rinsing etc., in case of re-entrant cavities[10].

3.1 Five-cell elliptical cavity

After the comparative study of the single-cell cavities of different shapes, the simulation of 5-cell elliptical cavity as shown in Fig. 3 for 650 MHz, β=0.61, has been carried out.

The plots of electric field lines for four non-accelerating modes, *i.e.,* π/5-mode (or 0-mode) to 4π/5-modes are shown in Fig. 4 and the fundamental accelerating mode (or π-mode) has been shown in Fig. 5 and the simulation results for two different five-cell elliptical cavities with same iris radius

Table 1 — Simulation results for single-cell elliptical and re-entrant cavities at 650 MHz, β=0.61

A/B (mm./mm.)	a/b (mm./mm.)	Equator radius D/2 (mm.)	Iris radius R_{iris} (mm.)	Half-Cell Length L/2 (inner) (mm.)	R/Q (Ω)	G(=Q.R_s) (Ω)	E_{acc} (MV/m)	E_{pk}/E_{acc}	B_{pk}/E_{acc} [mT/ (MV/m)]	$f_{\pi\text{-mode}}$ (MHz)	Remarks
54/58	13.7/ 30.876	197.346	48	70.335	58.6	192.9	17.0	3.048	4.7172	650.008	2D SUPERFISH, 3D CST MWS, α = 2.38 deg. Energy = 23.87 J, (Elliptical cavity)
65/54	13.67/ 30.8	188.1	48	70.335	63.2	202.5	17.0	3.085	4.525	650.008	2D SUPERFISH, 3D CST MWS, α = −10.48 deg. Energy = 22.13 J, (Re-entrant cavity)

(48 mm.) have been presented in Table 2. The said accelerating cavities are designed to achieve accelerating gradient of 17 MV/m.

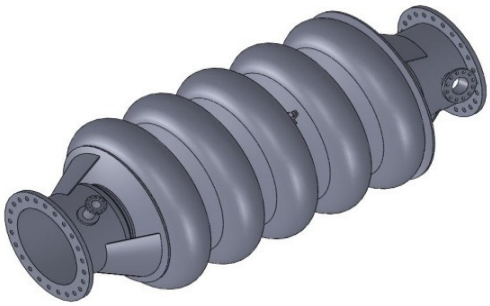

Fig .3 — Isometric view of 5-cell elliptical cavity

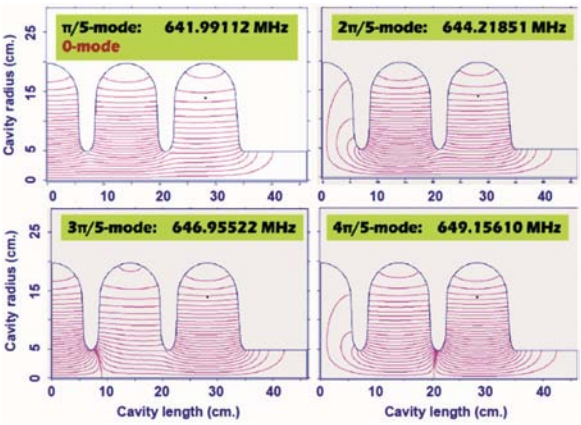

Fig. 4 — Plot of electric field lines for π/5 mode (0-mode), 2π/5, 3π/5 and 4π/5 modes of elliptical shape, 5-cell cavity (1/4 th geometry shown), [CAVITY-1]

CAVITY-1 has uniform wall slope angle (α) of 3.6 degrees in all half cells, but the equator ellipse aspect ratio (A/B) and iris ellipse aspect ratio (a/b) for the end-cells are different from that of the mid cells. CAVITY-2 has α = 2.4 degrees in all mid-cells and 4.5 degrees in the two end-cells, but (a/b) for the end-cells are different from that of the mid cells with (A/B) kept unchanged for all cells.

It is observed from Table 2 that all *RF* parameters for CAVITY-2, are better than those for CAVITY-1. As desired, the values of B_{pk}/E_{acc} and E_{pk}/E_{acc} for CAVITY-2 are little lower than those values for CAVITY-1.

The iris radius (R_{iris}) is a very powerful knob to trim *RF* parameters. B_{pk}/E_{acc} and E_{pk}/E_{acc} both increase as the iris radius (R_{iris}). But the increase of E_{pk}/E_{acc} is

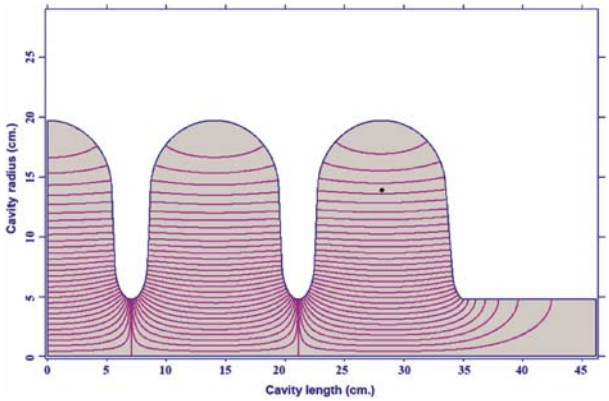

Fig. 5 — Plot of electric field lines for accelerating mode (π-mode) elliptical shape 5-cell cavity (1/4 th geometry shown) [CAVITY-1]

Table 2 — Simulation results for five-cell elliptical cavities at 650 MHz, β=0.61

A/B (mm./mm.)	a/b (mm./mm.)	Equator radius D/2 (mm.)	Iris radius R_{iris} (mm.)	Half-Cell Length L/2 (inner) (mm.)	R/Q (Ω)	G (=Q.R_s) (Ω)	E_{acc} (MV/m)	E_{pk}/E_{acc}	B_{pk}/E_{acc} [mT/(MV/m)]	$f_{\pi\text{-mode}}$ (MHz)	Remarks
54/58	11.99/27	198.175	48	70.335	290	197	17.0	3.34	4.90	650	2D SUPERFISH, 3D CST MWS, $(a/b)_{end}$=20.66/46.54 $(A/B)_{end}$=45.94/49.35 α = 3.6 deg. for all half cells Energy = 118.8 J Mesh size=0.05
54/58	13.68/30.82	197.40	48	70.335	296	200	17.0	3.00	4.84	650	2D SUPERFISH, 3D CST MWS, α = 2.4 deg. (mid-cells) = 4.5 deg. (end-cells), $(a/b)_{endcell}$=10.67/24.02 $(A/B)_{end}$= 54/58 Energy = 118.8 J Mesh size=0.05

much faster than that of B_{pk}/E_{acc}. However, the value of R/Q decreases as the iris radius as shown in Fig. 6 and consequently the *RF* power loss and hence the thermal load on the cryogenic system increases with iris aperture. So, the smaller iris aperture (R_{iris}) is preferable because of higher R/Q value and lower B_{pk}/E_{acc} and E_{pk}/E_{acc} values.

For the mid-cells, the maximum accelerating gradient (E_{acc}) increases with iris radius (R_{iris}) as shown in Fig. 7. However, for the two end-cells, the maximum E_{acc} decreases with R_{iris} and the field flatness is not maintained. So the optimized value of R_{iris} is 48 mm. in this case. Besides this, proper end-cell tuning is done to achieve better field flatness throughout all cells. In this case, for end cells the iris ellipse ratio is optimized to $(a/b)_{endcell}$=10.67/24.02 as compared to 13.68/30.82 for mid-cells. However, the equator ellipse ratio(A/B)=54/58 remained constant for both mid-cells and end-cells. But, the wall slope angle for end-cells is optimized to $\alpha_{endcell}$ = 4.5 degree as compared to 2.4 degree for mid-cells. The different geometry of end-cells require a different die from that of mid-cells.

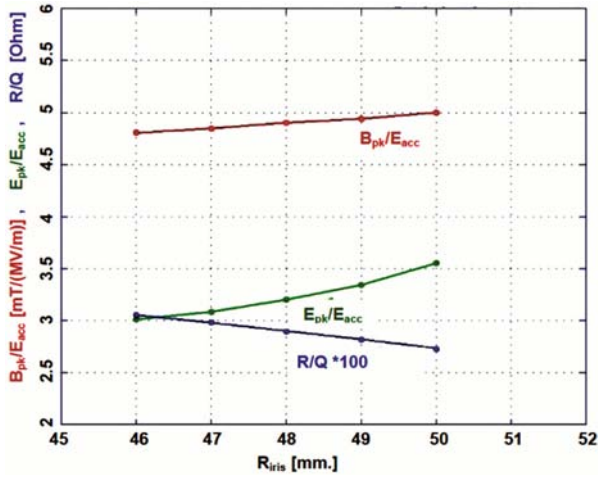

Fig. 6 — Plot of B_{pk}/E_{acc}, E_{pk}/E_{acc} and R/Q versus R_{iris} [for CAVITY-1]

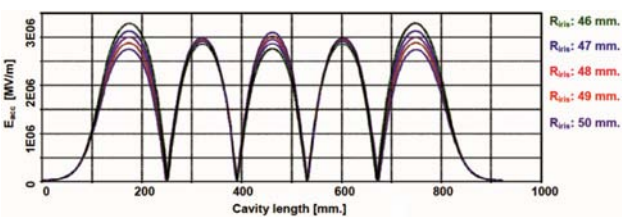

Fig. 7 — Plot of accelerating gradient (E_{acc}) along the cavity axis for different iris radius (R_{iris}) [for CAVITY-1]

The variation of equator radius ($R_{equator}$) has a very little effect on electromagnetic parameters as shown in Fig. 8 like, B_{pk}/E_{acc}, E_{pk}/E_{acc} and R/Q. Also, the maximum accelerating gradient (E_{acc}) on the axis throughout the 5-cell cavity almost unchanged with the variation of the equator radius. The field flatness does not depend on the variation of the equator radius ($R_{equator}$).

A plot of transit time factor versus β for 650 MHz, β=0.61, 5-cell SCRF cavity is shown in Fig. 9. It is observed that the said cavity with geometric β~0.61 can accept wider β value (0.56 to 0.8) obtained with no end cells tuning than the β value (0.57 to 0.75) obtained with end cells tuning done.

A plot of B_{pk}/E_{acc} versus equator ellipse aspect ratio (Fig. 10) shows that B_{pk}/E_{acc} is almost unchanged

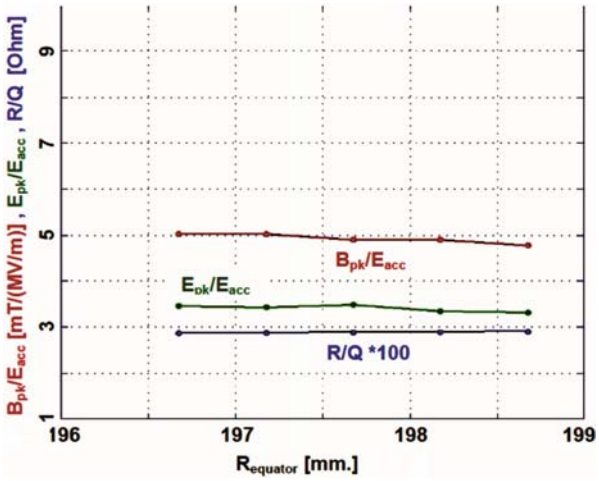

Fig. 8 — Plot of B_{pk}/E_{acc}, E_{pk}/E_{acc} and R/Q vs. $R_{equator}$ [for CAVITY-1]

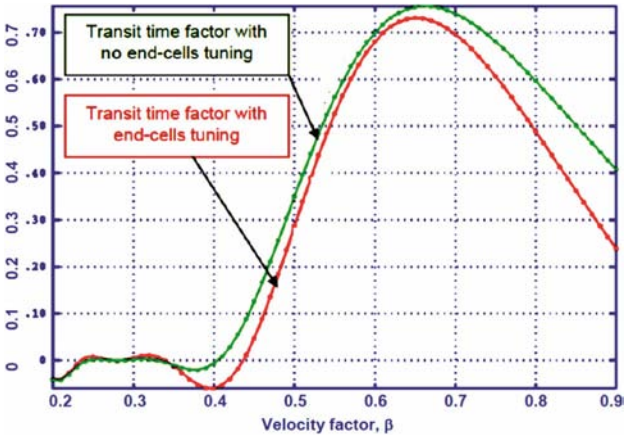

Fig. 9 — Plot of transit time factor versus β for 650 MHz, β=0.61, 5-cell SCRF cavity [for CAVITY-1]

i.e., varies between 4.82 and 4.9 mT/(MV/m) as equator ellipse aspect ratio, A/B. However, the value of B_{pk}/E_{acc} varies as shown in Fig. 11 from 5.2 to 4.7 mT/(MV/m) as iris ellipse aspect ratio, a/b and it has a minimum value of 4.6 mT/(MV/m) at a/b=0.5.

It is observed that E_{pk}/E_{acc} increases from 2.9 to 3.9 as shown in Fig. 12 as equator ellipse aspect ratio, A/B. However, the value of E_{pk}/E_{acc} decreases as shown in Fig. 13 from 3.5 to 3.0 with the increase of iris ellipse aspect ratio, a/b.

Finally, after analyzing all pros and cons between CAVITY-1 and CAVITY-2 and also considering the better field flatness factor, the design of CAVITY-2 has been frozen as the best one. The engineering drawings for the half-cell of mid-cells and end-cells of CAVITY-2 are shown in Figs 14 and 15, respectively.

A comparative chart of design parameters from three different laboratories, Jefferson Lab (JLab), Fermilab and VECC for five-cell elliptical cavities at 650 MHz, β=0.61 is presented in Table 3. It is observed that JLab design has larger iris radius of 50 mm. in comparison to 42 mm of Fermilab and 48 mm. of VECC. The larger iris radius will increase cell-to-cell coupling coefficient as well as peak surface electric and magnetic fields. Jlab design has some flat equator region. But, Fermilab and VECC designs do not have any such region. The wall slope angle for JLab design is 0 degree (for both mid-cells and end-cells) as compared to 2 degree (mid-cells) and 2.7 degree (end-cells) in case of Fermilab and

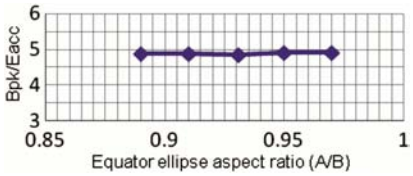

Fig. 10 — Plot of E_{pk}/E_{acc} versus A/B [for CAVITY-2]

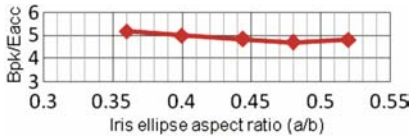

Fig. 11 — Plot of E_{pk}/E_{acc} versus a/b [for CAVITY-2]

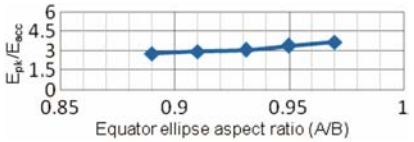

Fig. 12 — Plot of E_{pk}/E_{acc} versus A/B [for CAVITY-2]

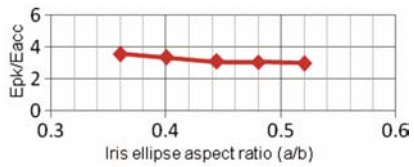

Fig. 13 — Plot of E_{pk}/E_{acc} versus a/b [for CAVITY-2]

Table 3 — Comparative chart of design parameters[13] for five-cell elliptical cavities at 650 MHz, β=0.61

Name of the lab designed	A/B (mm./mm.)	a/b (mm./mm.)	Equator radius D/2 (mm.)	Iris radius R_{iris} (mm)	Half-Cell Length L/2 (inner) (mm.)	R/Q (Ω)	G (=Q.R_s) (Ω)	E_{acc} (MV/m)	E_{pk}/E_{acc}	B_{pk}/E_{acc} [mT/(MV/m)]	$f_{\pi\text{-mode}}$ (MHz)	Remarks
Fermilab (FNAL)	54/58	14/25	194.95	42	70.335	378	191	17.0	2.26	4.21	650	2D SLANS code L/2 = 71.385 (end-cell) α = 2.0 deg. (mid-cell) = 2.7 deg. (end-cell) E = 92.7 J
Jefferson Lab (JLAB)	50.46/45	15/22	192.10	50	65.456	297	190	17.3	2.71	4.78	650	2D SUPERFISH code Equator flat = 0.976 mm.(mid-cell) = 0.5047 (end-cell) α = 0 degree E = 118.8 J
VECC	54/58	13.68/30.82	197.40	48	70.335	296	200	17.0	3.00	4.84	650	2D SUPERFISH, 3D CST MWS, α = 2.4 deg. (mid-cells) = 4.5 deg. (end-cells), $(a/b)_{endcell}$=10.67/24.02 Energy = 118.8 J

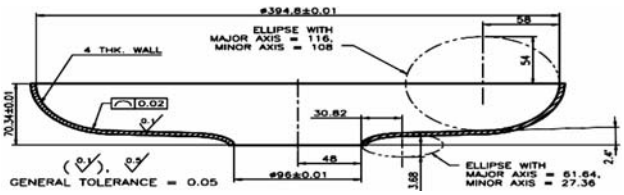

Fig. 14 — Engineering drawing for half-cell (mid-cell) of CAVITY-2

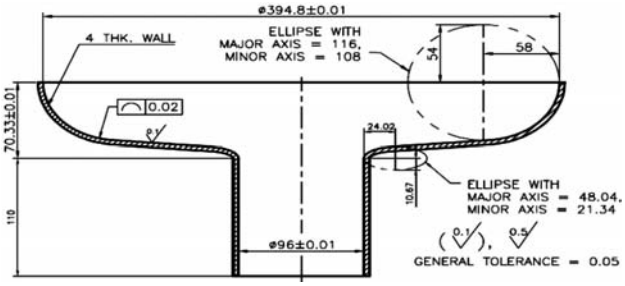

Fig. 15 — Engineering drawing for half-cell (end-cell) of CAVITY-2

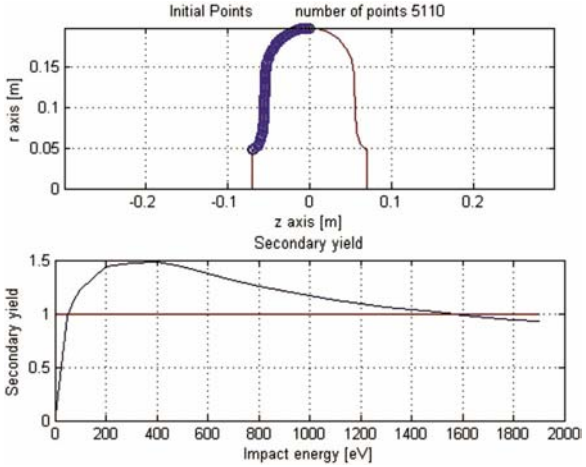

Fig. 16 — Input for mid-cell of the 5-cell cavity

2.4degree (mid-cells) and 4.5 degree (end-cells) in case of VECC design. So, for JLab design, the same die can be used for mid-cells and end-cells. However, for Fermilab and VECC designs, the different die will be required for mid-cells and end-cells. There are little difference in equator and iris ellipse aspect ratios among the three designs.

4 Multipacting

A preliminary study of multipacting analysis for 650 MHz, β=0.61, 5-cell SCRF cavity has been carried out using 2D code MultiPac2.1 (Windows version). The analysis has been done for both mid-cells and end-cells and the inputs for mid cells and end cells are shown in Figs 16 and 17. The secondary electron emission coefficient is greater than 1, if the impact energy of electron is above 50 eV. In the present multipact analysis, 30 impacts of electrons have been considered, which is a sufficient proposition for analysis.

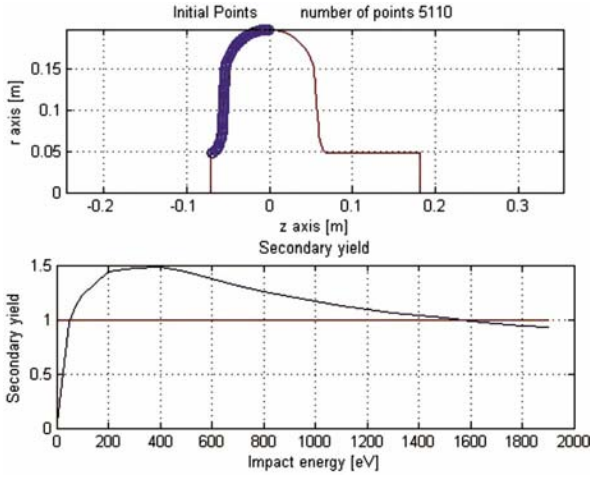

Fig. 17 — Input for end-cell of the 5-cell cavity

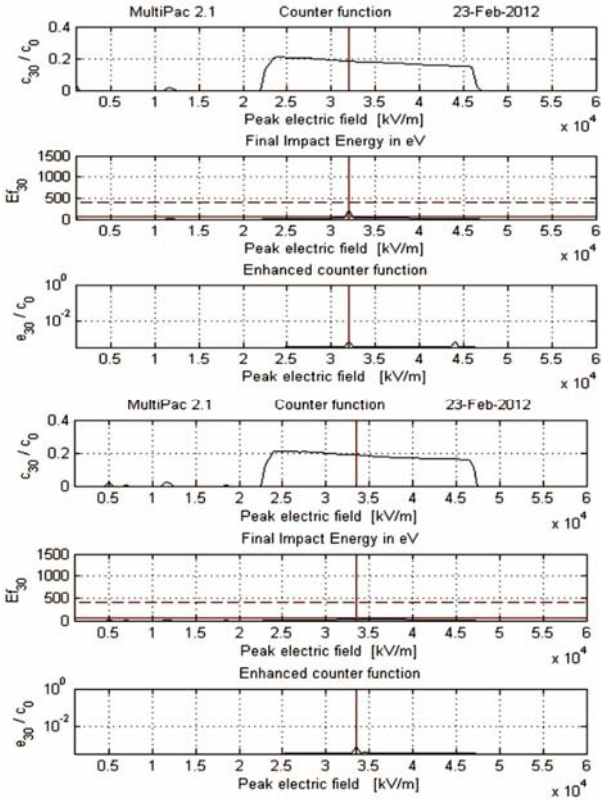

Fig. 18 — Plot of electron counter function, impact energy and enhanced electron counter function with peak electric field for (a) mid-cell and (b) end-cell of the 5-cell cavity

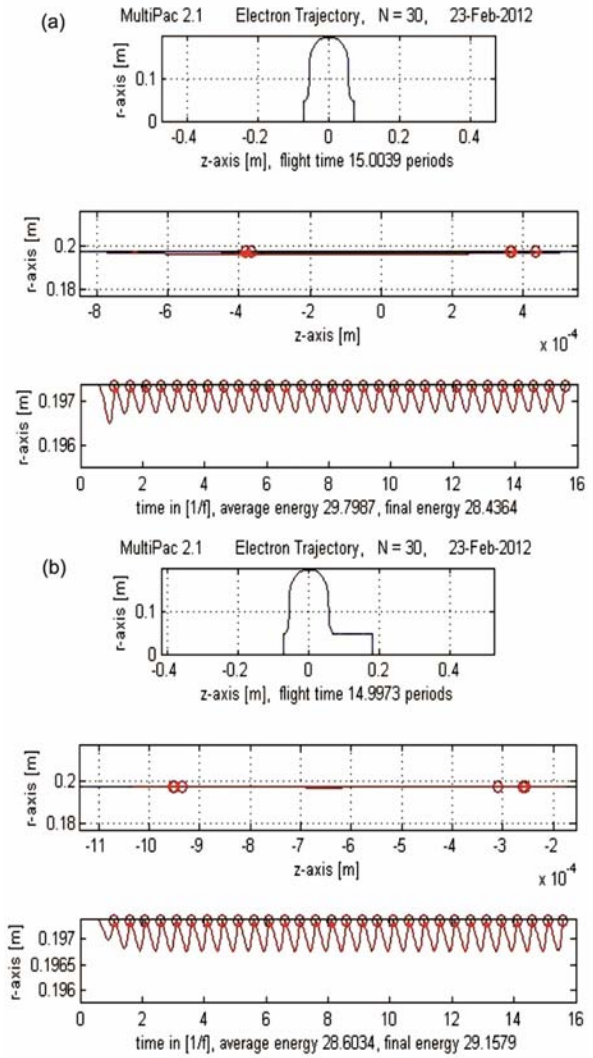

Fig. 19 — Plot of electron impact at the equator region (zoomed scale) with *RF* period for (a) mid-cell and (b) end-cell of the 5-cell cavity.

The result of the multipacting analysis for the mid-cell and end-cell of the said cavity is discussed below. Figure 18(a) & (b) shows the variation of three parameters, electron counter function (c_{30}/c_0), average impact energy (Ef_{30}) and enhanced electron counter function (e_{30}/c_0), with peak electric field for mid-cell and end-cell cavities, respectively.

The c_0 is the initial number of electrons which can impact on the surface of the cavity, c_{30} is the total number of electrons (with and/or without proper impact energy and phase synchronization to cause multipacting) available after 30 impacts on the surface of the cavity and e_{30} is the number of secondary electrons (with proper impact energy and phase synchronization to cause multipacting). The impact energy is less than 50 eV for all peak electric fields except a small region between 30–35 MV/m, where it is around 200 eV. However, we can conclude that no multipacting can take place in the said cavity as the relative enhanced electron counter function is less than 1 for the whole range of peak electric field up to 60 MV/m.

It is observed from Fig. 19(a) & (b) for mid-cells and end-cells that even after 30 impacts of electrons at the equator region (at the radius of 197 mm.) of the cavity, the final impact energy is 28.4364 eV, which is well below 50eV and hence,it is unlikely to cross secondary electron emission yield for producing multipacting.

5 Conclusions

An approach has been made for the design of single cell and 5-cell SCRF cavities of 650 MHz, β=0.61 for proton accelerator. The design of cavities for electron accelerator[11] was not in the scope of this paper. A comparative study between different shapes of cavity has been discussed in this paper and optimized the various *RF* design parameters. The different computer codes like, 2D SUPERFISH, 3D Microwave Studio, have been used for the purpose and the results obtained from these codes had a little deviation between each other for the same geometry and mesh sizes. CAVITY-2 has been taken as the optimized 5-cell, β=0.61, 650 MHz SCRF cavity. The multipacting analysis with 2D MultiPac2.1 code shows that the possibility of multipacting is negligible. However, further analysis with 3D CST Particle Studio code, in which Furman model[12] of secondary emission including true, elastic and rediffused secondary electrons, is being carried out for final assessment. A comparative study of the design parameters for three designs of JLab, Fermilab and VECC has been made and VECC design is good enough and comparable to that of Jlab and Fermilab design.

Acknowledgement

The author would like to thank Mr A. Duttagupta, MEG, VECC for helping us to make engineering drawing of the cavity half cell.

References

1 Geng R L, *Proceedings of International Particle Accelerator Conference*, (PAC07), New Mexico, USA, (2007) 2337.
2 Kneisel P, *RF Superconductivity*, (France) (1995) 449.

3 Padamsee H, *RF Superconductivity for accelerators* (John Willey & Sons Inc) (1998).
4 Pagani C, *RF Superconductivity, Tsukuba* (Japan) (2001) 115.
5 Graber J, *Nucl Instrum & Methods in Phys Res A*, 350 (1994) 572.
6 Geng R L, *Physica C Superconductivity*, 441 (2006) 145.
7 Kneisel P, *Proceedings of European Particle Accelerator Conference* (EPAC 2002), Paris, France, (2002) 139.
8 Aune B, *Physical Review Special topics-Accelerators & Beams*, 3 (2001) 092001.
9 Som S, *Proceedings of Indian Particle Accelerator Conference* (IUAC, New Delhi, India) (2011).
10 Geng R L & Padamsee H, *Proceedings of the Workshop on pushing the limits of RF Superconductivity* (ANL, USA) (2004).
11 Mittal K C, *Indian J Pure & Appl Phys*, 50 (2012) 772.
12 Furman M A & Pivi M T F, *Physical Review Special Topics Accelerators Beams*, 5 (2002) 1244004.
13 Som S, *Proceedings of the 16th Workshop on RF Superconductivity* (Paris, France) (2013) 1193.